Heliyon 9 (2023) e20747

Contents lists available at ScienceDirect

Heliyon

journal homepage: www.cell.com/heliyon

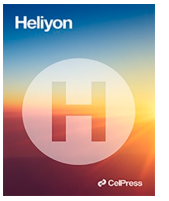

Anti-cervical cancer mechanism of bioactive compounds from *Alangium platanifolium* based on the 'compound-target-disease' network

Hao Zhang [a,b], Ruiming Zhang [b], Yuefen Su [b], Jingrou Zheng [b], Hui Li [b], Zhichao Han [b,c], Yunzhen Kong [b], Han Liu [b], Zhen Zhang [b], Chunmei Sai [b,*]

[a] College of Pharmacy, Weifang Medical University, Weifang, 261053, China
[b] College of Pharmacy, Jining Medical University, Rizhao, 276826, China
[c] College of Agriculture, Yanbian University, Yanji, 133002, China

ARTICLE INFO

Keywords:
Alangium platanifolium
Cervical cancer
Molecular docking
Molecular networking
Network pharmacology
UPLC-Q-TOF-MS

ABSTRACT

In this study, we analyzed the chemical compositions of *Alangium platanifolium* (Sieb. et Zucc.) Harms (AP) using ultraperformance liquid chromatography-quadrupole time-of-flight mass spectrometry (UPLC-Q-TOF-MS) non-targeted plant metabolomics integration MolNetEnhancer strategy. A total of 75 compounds, including flavonoids, alkaloids, terpenes, C_{21} steroids, among others, were identified by comparing accurate mass-to-charge ratios, MS^2 cleavage fragments, retention times, and MolNetenhancer-integrated analytical data, and the cleavage rules of the characteristic compounds were analyzed. A total of 125 potential cervical cancer (CC) therapeutic targets were obtained through Gene Expression Omnibus (GEO) data mining, differential analysis, and database screening. Hub targets were obtained by constructing protein-protein interaction (PPI) networks and CytoNCA topology analysis, including SRC, STAT3, TP53, PIK3R1, MAPK3, and PIK3CA. According to Gene ontology (GO) analysis, AP was primarily against CC by influencing gland development, oxidative stress processes, serine/threonine kinase, and tyrosine kinase activity. Enrichment analysis of the Kyoto Encyclopedia of Genes and Genomes (KEGG) indicated that the PI3K/AKT and MAPK signaling pathways play a crucial role in AP treatment for CC. The compound-target-pathway (C-T-P) network revealed that quercetin, methylprednisolone, and caudatin may play key roles in the treatment of CC. The results of molecular docking revealed that the core compound could bind significantly to the core target. In this study, the compounds in AP were systematically analyzed qualitatively, and the core components, core targets, and mechanisms of action of AP in the treatment of CC were screened through a combination of network pharmacology tools. Providing a scientific reference for the therapeutic material basis and quality control of AP.

1. Introduction

Cervical cancer (CC) is the fourth most frequent malignancy globally and the fourth principal cause of cancer-related mortality in women [1]. According to statistics, there were 604,127 new cases of CC and 341,831 deaths from CC globally in 2020 [2]. Current

* Corresponding author. College of Pharmacy, Jining Medical University, Rizhao, Shandong, China.
E-mail address: saichunmei1980@163.com (C. Sai).

https://doi.org/10.1016/j.heliyon.2023.e20747
Received 8 August 2023; Received in revised form 1 October 2023; Accepted 5 October 2023
Available online 6 October 2023

treatments for CC mainly include radiotherapy, chemotherapy, and/or surgical resection. However, these modalities can cause various adverse effects and have limited efficacy in advanced CC [3]. Therefore, identifying a safer and less toxic treatment strategy for the effective treatment of CC is crucial. Natural products have received widespread attention as a potential source of highly effective and low-toxicity antitumor drugs. There is increasing evidence that plant-derived natural products can achieve anti-CC effects through various mechanisms, including inhibition of CC cell proliferation, induction of CC apoptosis, reduction of telomerase activity, and inhibition of angiogenesis [4,5]. Based on previous literature research, *Alangium platanifolium* (Sieb. et Zucc.) Harms (AP) belonging to the family Alangiaceae is an important medicinal resource. In the "Quality Standards for Traditional Chinese Medicinal Materials and Ethnic Medicinal Materials in Guizhou Province (2003 Edition)" of China, it is explicitly stated that Bajiaofeng refers to the dried fine whisker roots or dry branches of the *Alangium chinense* (Lour.) Harms and the *Alangium platanifolium* (Sieb.et Zucc.) Harms. Recent studies have shown that monomeric compounds from *Alangium chinese* exhibit good inhibitory effects on HeLa cells [6]. The current research has placed significant emphasis on *Alangium chinense*, but insufficient with regards to AP. While a few glycosides have been extracted from its leaves, there is a dearth of information regarding the components of its root. To expand the potential applications of AP in medicinal contexts, it was selected as the primary focus of this study.

Based on liquid chromatography-mass spectrometry (LC-MS), non-targeted plant metabolomics is an indispensable method for decoding and synthetically characterizing phytochemical components. However, Given the large number and complex chemical components of primary and secondary metabolites in plants, LC-MS-based non-targeted plant metabolomics methods are not ideal for large-scale identification of the structure of various compounds in samples. To address this challenge, several advanced informatics tools have been developed in recent years to improve the annotation of compounds [7]. The Global Natural Products Social Molecular Networking (GNPS) serves as a platform designed to analyze and archive tandem mass spectrometry data, which can build nodes (compounds) with similar secondary mass spectrometry cleavage fragments (MS^2) into molecular networking based on the MS-Cluster algorithm. By comparing the node information in the network, it is helpful to identify similar compounds and discover novel compounds [8]. In addition, MolNetEnhancer is a workflow in the GNPS molecular networking analysis platform that integrates analysis results from the GNPS library matching, Mass2Motifs LDA parameters (MS2LDA), Network Annotation Propagation (NAP), and DEREPLICATOR+, as well as automatically chemically classified via ClassyFire. This *in-silico* mining tool significantly enhances the scope and efficiency of compound identification in complex natural products [9]. Currently, MolNetEnhancer has been used to improve the annotation of compounds in metabolites and to characterize the chemical space in plants [10,11].

Several effective phytochemical components may theoretically act on multiple targets and pathways. Network pharmacology is suitable for revealing the overall mode of action of multi-component, multi-target, and multi-pathway natural products, which can solve the problems of poor efficacy and drug resistance of single-target drugs [12]. Molecular docking is one of the important means of computer-aided drug design, which can predict the optimal conformation and binding sites between small molecules, express interactions in enzyme reactions, and predict and explain biological reaction mechanisms [13].

Herein, LC-MS-based non-targeted plant metabolomics coupled with the MolNetEnhancer strategy was applied to qualitatively analyze the components of methanol extracts of AP roots. In addition, the network pharmacological method combined with bioinformatics analysis was applied to identify key active ingredients, hub targets, and potential molecular mechanisms of AP against CC, and finally verified the binding effect of active compounds to hub targets through molecular docking.

2. Materials and methods

2.1. Materials and reagents

HPLC-grade acetonitrile was obtained from Honeywell Burdick & Jackson (New Jersey, USA). LC/MS-grade acetonitrile was obtained from Mallinckrodt Baker, Inc. (New Jersey, USA). HPLC-grade methanol was obtained from Sinopharm Chemical Reagent Co., Ltd. (Shanghai, China). Glacial acetic acid (GAA) was obtained from TEDIA. (Ohio, USA). The experimental water was purified by the Millipore water purification system (Massachusetts, USA).

In August 2021, AP roots, aged between 8 and 10 years, were freshly collected from a humid valley at an altitude of 1400 to 2000 m in Qujing, Yunnan Province, China. The sample was identified by Professor Jian'an Wang (School of Pharmacy, Jining Medical University). The voucher sample (GMG-20210815) was stored at 4 °C at Jining Medical University.

2.2. Sample preparation

The AP roots were left in a cool, well-ventilated area for 30 days to allow natural evaporation of water. Methanol is the preferred solvent for extracting the polar and moderately polar compounds, which are the specific compounds we are targeting [14]. Therefore, the crushed root powder of AP (20.00 kg) was thoroughly extracted with methanol 3 times by methanol cooling extraction for 7 days each. After vacuum concentration, a methanol crude extract was obtained.

The methanol extract of 200 mg of AP was precisely weighed, dissolved in 5 ml of methanol, then extracted ultrasound for 30 min (40 kHz, 200 W), and cooled to room temperature. The test solution was filtered once using a 0.22 μm microporous membrane for subsequent analysis.

2.3. UPLC-Q-TOF-MS analysis

The sample analysis used the Agilent 6530B Accurate Mass Q-TOF LC/MS System with an electrospray ionization source (ESI)

interface. A 4.6 × 150 mm TOSOH TSK gel ODS-100V column was used for chromatographic separations. The temperature of the column oven was maintained at 30 °C. The flow rate of the mobile phase was adjusted to 1.0 ml/min, and the injection volume was 5 μl.

The conditions for UPLC and MS were optimized. Mobile phase A is GAA aqueous solution with a concentration of 0.5 % (pH = 3) and mobile phase B is acetonitrile. Gradient parameters were set as follows: 10 % B, 0–15 min; 10–20 % B, 15–30 min; 20–30 % B, 30–40 min; 30–60 % B, 40–50 min; 60–80 % B, 50–60 min.

For qualitative analysis of ESI-MS, both positive and negative ion full scans were used to obtain more detailed ion information. Scanning mass-to-charge ratio (m/z) ranged from 100 to 1200. The nebulizer pressure was set to 45 psi and the capillary volt was set to (±) 3000 V. The drying gas flow rate was adjusted to 5 l/min and the drying gas temperature was set to 350 °C. In the auto MS/MS mode, the acquisition of MS/MS spectra occurred at a scan speed of 2 spectra per second.

The analysis data was preprocessed using Agilent MassHunter Qualitative Analysis B.06.00 software, including integration, smoothing, deconvolution, and isotope filtering.

2.4. Molecular networking and compound identification

The processed MS^2 data was converted to mzML format by ProteoWizard MSConvert, which was then uploaded to the UCSD GNPS mass spectrometry platform. MS^2 data were processed and filtered again during the creation of the METABOLOMICS-SNETS-V2. The value of the precursor ion mass tolerance (PIMT) was adjusted to 2.0 Da and the value of the fragment ion mass tolerance (FIMT) was adjusted to 0.5 Da. The remaining parameters were set to their default values.

MS/MS data were decomposed into annotated Mass2Motifs using the MS2LDA tool [15]. Dereplication was performed using the DEREPLICATOR + algorithm tool to identify more compounds [16]. NAP was able to build molecular networks based on the principle of spectral similarity and then improved the annotation of small molecules using *in silico* fragmentation predictions [17]. The completed GNPS molecular network, MS2LDA, and DEREPLICATOR+ were integrated using MolNetEnhancer, analyzed online on the GNPS platform, and visualized using Cytoscape 3.9.1.

2.5. Screening of compounds in AP by ADME druggability evaluation

Compounds in AP were pharmacokinetically screened using SwissADME [18]. SwissADME is widely for evaluating the druggability of small molecule compounds in natural products [19,20]. The screening criteria for potential active compounds were: (1) Gastrointestinal (GI) absorption was 'High'; (2) two or more of the five types of medicinal properties (Lipinski, Ghose, Veber, Egan, Muegge) results were 'yes'.

2.6. Screening of targets of active compounds in AP

Predicted targets of active compounds were acquired through three online databases, including Swisstargetprediction, DrugBank, and BATMAN-TCM. The collected targets were normalized by using the UniProt database, the species was limited to 'Homo sapiens', and duplicate values were removed.

2.7. Screening of CC-related targets

Three CC-related chip data were downloaded from the GEO database: GSE26342 (NIAID GPL1052 Platform-NIAID-Hsaa, GPL1053 Platform-NIAID-Hsab), GSE63514 (Affymetrix GPL570 Platform-HG-U133_Plus_2), GSE173097 (Agilent GPL16956 Platform-Agilent-045997 Arraystar human lncRNA microarray V3). Details of all GSE chip datasets were shown in Table 1.

The R programming language 4.3.0 and the R package 'limma' were applied to acquire differentially expressed genes (DEGs) in each GSE dataset. A p-value <0.05 and $|\log(\text{fold change})| > 1$ were used as restriction criteria for sifting differential genes. The R packages "ggplot2" and "pheatmap" were applied to construct volcano plots and heatmaps of the DEGs, respectively. Robust Rank Aggregation (RRA) is a commonly used bioinformatics tool that comprehensively ranks genes from different data sources [24]. The RRA algorithm was employed to integrate and analyze the three data sets to obtain significant DEGs as potential targets for CC. CC-associated targets were also acquired from the DrugBank, OMIM, GeneCards, PharmGKB, and TTD databases.

All obtained CC-related targets were standardized by using the UniProt database. Finally, the R package 'VennDiagram' was applied to analyze the potential protein targets of AP against CC.

Table 1
Information of the three GSE datasets.

GEO	Platform	Samples(number) Total CC Control	Experiment type	Attribute	Author/reference
GSE26342	GPL1052 GPL1053	54 34 20	Array	Test	Mine, K.L [21]
GSE63514	GPL570	128 28 24	Array	Test	den Boon, J.A [22]
GSE173097	GPL16956	11 5 6	Array	Test	Shang, C.L [23]

2.8. Protein-protein interaction (PPI) networks

Possible potential interactions between potential therapeutic targets were explored on the STRING database. Parameters were set as follows: only targets belonging to the species "Homo sapiens" were considered, a minimum interaction threshold of greater than 0.9 was set, and nodes that were not connected to the network were removed. Cytoscape 3.9.1 software was used to analyze and visualize the resulting PPI networks. Using CytoNCA, the node topology parameters were calculated, and crucial targets were identified.

2.9. GO and KEGG pathway enrichment analyses

The GO and KEGG enrichment analyses were conducted using the R language and associated R packages “clusterProfiler”, “stringr”, “AnnotationDbi”, “org. Hs.eg.db”, “DOSE”, “ggplot2” and “ggrepel”. The pvalueCutoff was 0.05 and the qvalueCutoff was 0.2, and only GO and KEGG analysis results with a p-value of <0.05 were retained.

2.10. The construction of a C-T-P network

The C-T-P network was constructed by importing data for potential therapeutic targets, active compounds, and top 30 signaling pathways into Cytoscape 3.9.1. Core compounds were screened based on Degree values in the network.

2.11. Molecular docking

The top 6 target proteins with the highest CytoNCA scores in the core PPI network were selected as receptors, and compounds that met pharmacokinetic screening were selected as ligands. The core targets were acquired from the Protein Data Bank (PDB) in three-dimensional (3D) format. Non-protein molecules in the core targets were removed by the Pymol 2.5. The core targets were

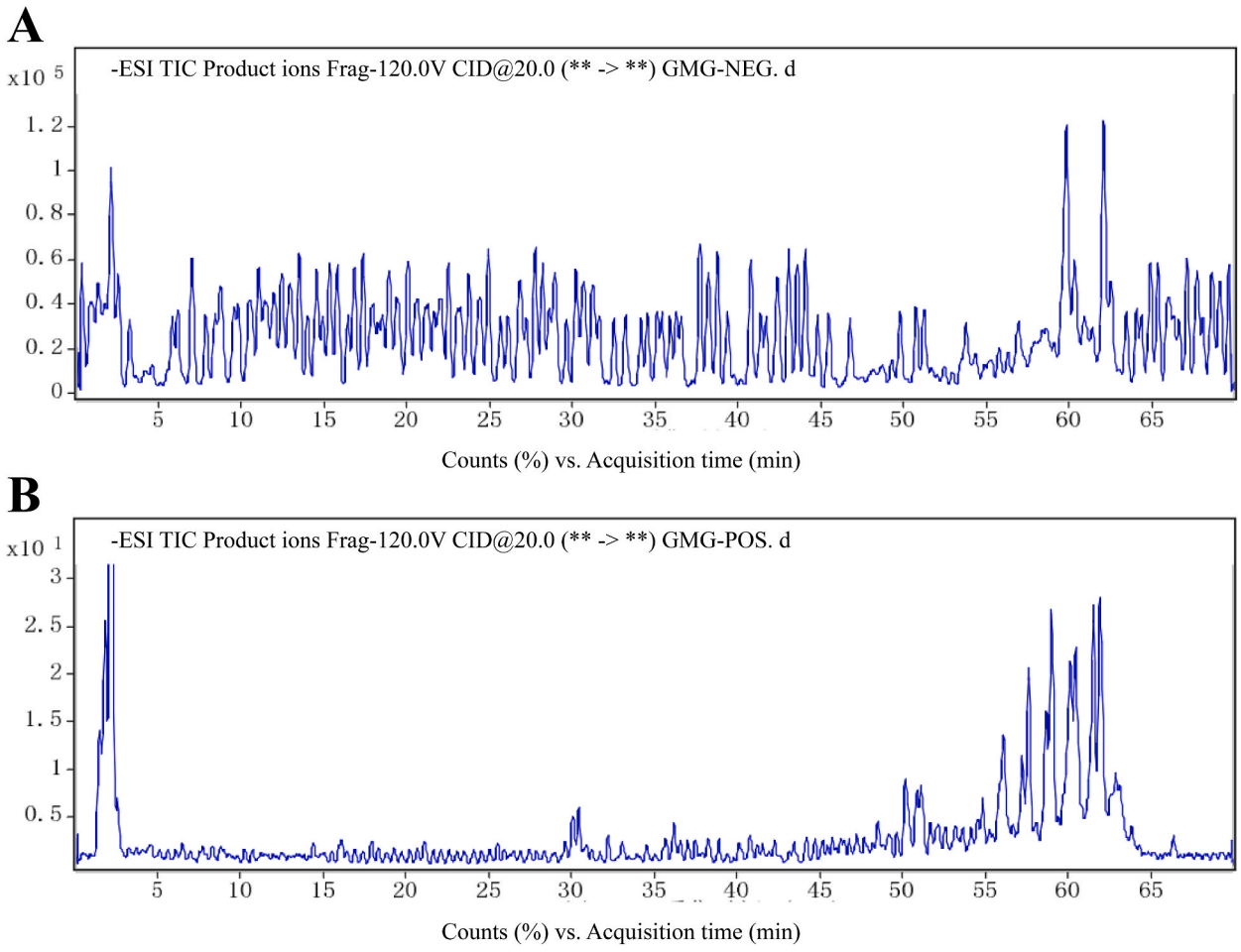

Fig. 1. TICs of methanol extracts of AP roots based on UPLC-Q-TOF-MS analysis. (**A**) TIC in the negative ESI mode. (**B**) TIC in the positive ESI mode.

hydrogenated using AutoDock Tools 1.5.7 and converted into the pdbqt file format for use as docking receptors. The two-dimensional (2D) structure of active compounds was drawn by ChemDraw 2019, and energy minimization was implemented by Chem3D 2019 and saved as a PDB file format. The active compounds were converted by Auto-Dock Tools 1.5.7 to a pdbqt file format for use as docking ligands.

Molecular docking was run via AutoDock Vina, the results were visualized using Discovery Studio 2021 Client software, and heatmaps of molecular docking data were drawn using R and the R package 'pheatmap'.

3. Results

3.1. Sample preparation

The methanol extracts of AP roots were concentrated to about 1.79 kg, the estimated dry paste amount was 1.19 kg, and the dry paste extraction rate was 5.97 %.

3.2. UPLC-Q-TOF-MS analysis

High-resolution mass spectrometry data of AP roots methanol extracts in positive and negative ion modes were acquired by the UPLC-Q-TOF-MS system, and their total ion chromatograms (TICs) were shown in Fig. 1. UPLC-Q-TOF-MS analysis showed that the methanol extract of AP was rich in chromatographic peaks in positive and negative ionization modes, making it ideal for comprehensive characterization of composition.

3.3. Molecular networking and compound identification

The family of structurally related molecules in AP was revealed by MolNetEnhancer. As shown in Fig. 2A, approximately 34.1 % of the MS^2 spectral matching nodes were classified as organoheterocyclic compounds, 7.5 % as lipids, and 5.2 % as phenylpropane and polyketones, etc.

A total of 252 nodes were generated by MolNetEnhancer in (+)-ESI and (−)-ESI-based modes, of which 137 nodes were clustered into 19 independent molecular families, and spectra not aggregated into molecular families were represented as self-ring nodes at the bottom of the network. A total of 28 matched compounds were obtained by GNPS library alignment. A total of 5 compounds were identified using *in silico* fragmentation graph by DEREPLICATOR+. Mass fragment peaks and/or neutral losses (Mass2Motif) were discovered by using MS2LDA annotation. There were 248 nodes (~98 %) labeled according to the 217 Mass2Motifs mapped to MS2LDA. NAP was used to perform *in silico* fragmentation prediction and 80 MetFrag, 38 Fusion, and 74 Consensus candidates were obtained. The partial results of the compounds identified by NAP-integrated MS2LDA were shown in Fig. 2B. Web links to data analysis result from GNPS libraries, MS2LDA, NAP, DEREPLICATOR+, and MolNetEnhancer were presented in Table S1.

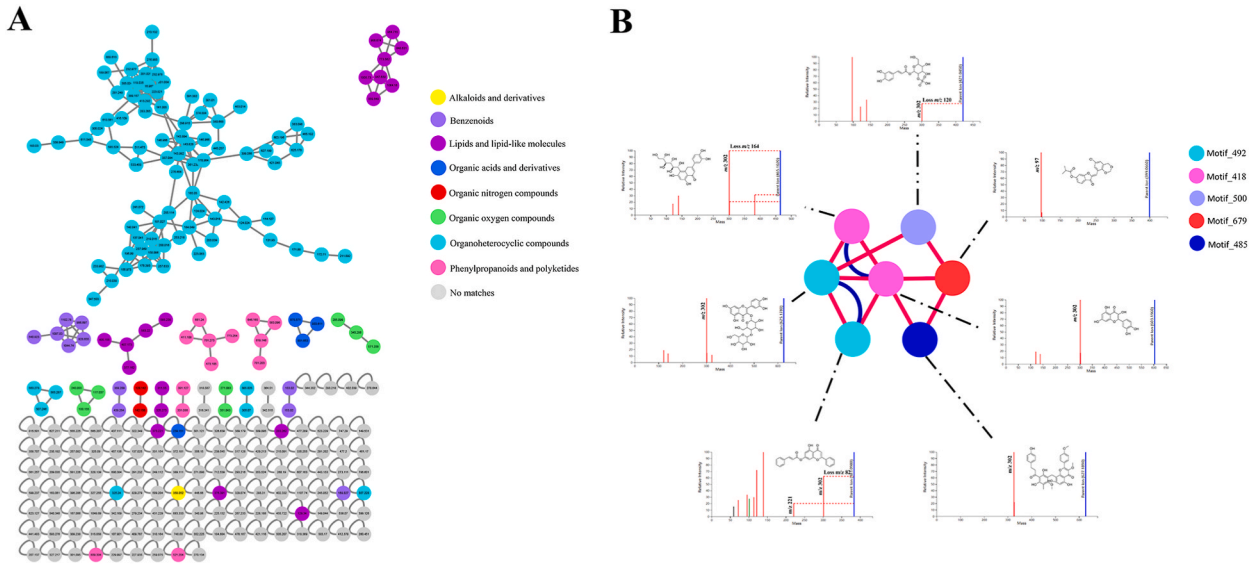

Fig. 2. Chemical classification and structural identification of methanol extracts of AP roots. (A) Nodes annotation using MolNetEnhancer combined with GNPS molecular network, MS2LDA, NAP, and DEREPLICATOR + output. The same color in the node represented the same family of molecules. (B) Characterize compounds using GNPS molecular network and NAP, combined with Mass2Motifs generated by MS2LDA. The same color represented the same Mass2Motifs. (For interpretation of the references to color in this figure legend, the reader is referred to the Web version of this article.)

A total of 75 compounds were identified by comparing accurate mass-to-charge ratios, MS^2 cleavage fragments, retention times, and MolNetenhancer-integrated analytical data. (Fig. 3). Based on their distinct structural types, the identified compounds can primarily be categorized into various groups, including flavonoids, alkaloids, terpenes, C_{21} steroids, organic acids, among others. Details of the 75 identified compounds are presented in Table S2.

3.4. Mass spectral fragmentation behavior

A total of fifteen alkaloids were identified, among which the excimer ion peak of the aporphine alkaloids in the positive ESI-MS mode was present in the form of $[M+H]^+$. When nitrogen methyl groups were present in the structure, it was easy to neutrally lose substituents such as NH_2CH_3 and $NH(CH_3)_2$, and the molecular loss of CH_3 and CH_4 will also occur, which is easy to produce characteristic fragment ions of *m/z* 279.10. Compound 15 (Duguetine N-oxide) was used as a representative expound. In the positive ESI-MS mode, the excimer ion peak was *m/z* 372.18 $[M+H]^+$ and secondary MS fragment ions were *m/z* 325.14 $[M + H–CHO_2]^+$, *m/z* 294.13 $[M + H–CHO_2–CH_3O]^+$, *m/z* 279.10 $[M + H–CHO_2–CH_3O–CH_3]^+$, and *m/z* 312.14 $[M + H–CHO_2N]^+$. Possible cleavage pathways of Duguetine N-oxide are shown in Fig. 4A.

A total of seven flavonoids were identified, among which the excimer ion peaks of flavonoids in both positive and negative ESI-MS modes exist as $[M+H]^+$ and $[M - H]^-$ peaks, respectively. The fragment ion fracture was mainly based on the removal of glycogenic ions and CO and H_2O, and the C ring was prone to RDA cleavage reaction. Compound 1 (Quercetin) was used as a representative expound. In the negative ESI-MS mode, the excimer ion peak was *m/z* 301.03 $[M - H]^-$, its secondary MS fragment ion was *m/z* 179.00 $[M\text{-}H\text{-}C_6H_5O_2]^-$ and 151.00 $[M\text{-}H\text{-}C_8H_6O_3]^-$. The possible lysis pathway of quercetin is shown in Fig. 4B.

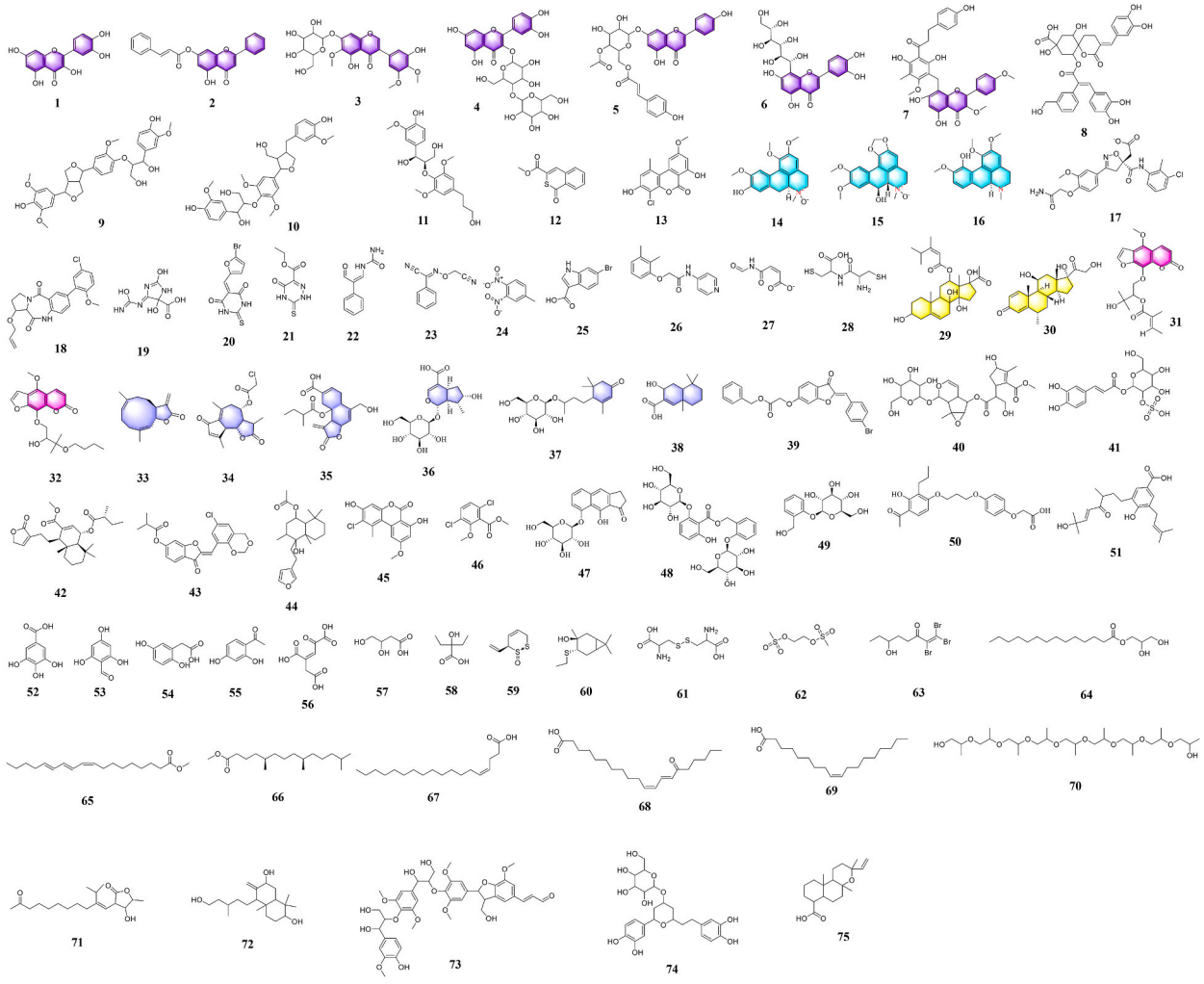

Fig. 3. Identified compounds from the methanol extracts of AP roots by GNPS and NAP.

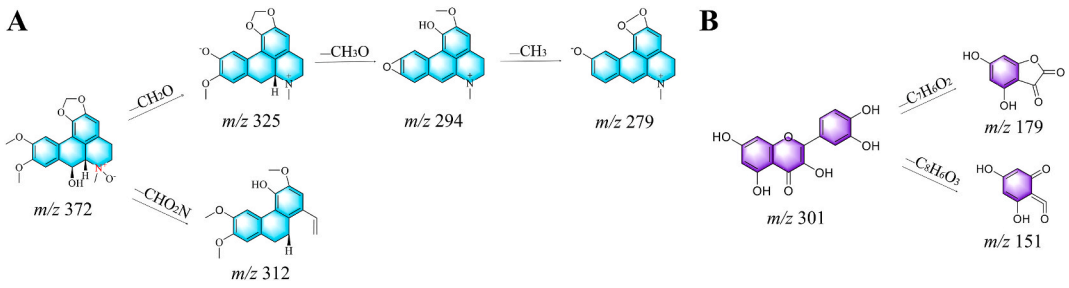

Fig. 4. Mass spectral fragmentation behavior of some characteristic compounds. (**A**) Cleavage pathways of Duguetine N-oxide. (**B**) Cleavage pathways of quercetin.

3.5. Screening of active ingredient by ADME druggability evaluation

Through SwissADME screening, 52 compounds were identified based on the selected criteria. The screening results are shown in Table S3. These 52 compounds were used for subsequent target determination.

3.6. Screening of targets of active compounds in AP

Through an extensive search on the Swisstargetprediction, DrugBank, and BATMAN-TCM databases, 41 compounds were identified as having targets. After removal of duplicate values and standardizing the collected targets, 914 unique targets were obtained (Table S4).

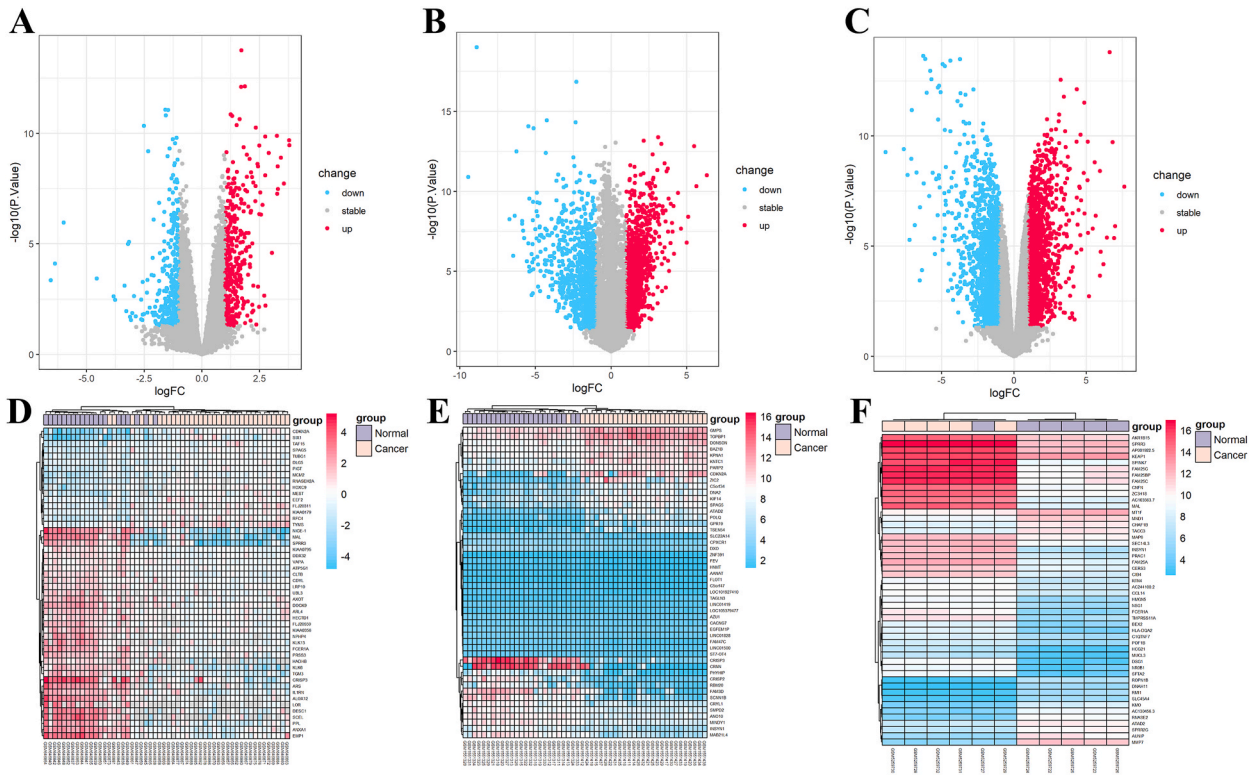

Fig. 5. Volcano plots of DEGs between normal group samples and disease group samples in three GSE microarray datasets. (A) GSE26342, (B) GSE63514 and (C) GSE173097. Red represents up-regulated genes and blue represents down-regulated genes. Heatmaps of the top 50 DEGs sorted by P value in three GSE microarray datasets. (D) GSE26342, (E) GSE63514 and (**F**) GSE173097. (For interpretation of the references to color in this figure legend, the reader is referred to the Web version of this article.)

3.7. Screening of CC-related targets

A total of 379, 1225, and 1940 upregulated genes were obtained sequentially in the GSE26342, GSE63514, and GSE173097 chip datasets based on difference analysis. Similarly, a total of 346, 1135, and 1940 down-regulated genes were obtained sequentially in the GSE26342, GSE63514, and GSE173097 chip datasets. Normalizations of gene expression were shown in Fig. S1.

Volcano plots of differential genes from three GEO chip datasets were shown in Fig. 5A–C. Heatmaps of the top 50 DEGs sorted by P-value in the three GEO chip datasets were shown in Fig. 5D–F. 32 integrated DEGs, including 16 significant up-regulated and 16 significant down-regulated genes, were acquired based on RRA (Table 2, Fig. 6).

The keyword "Cervical Cancer" was searched in several databases including GeneCards, DrugBank, OMIM, PharmGKB, and TTD. Following the standardizing of the targets, 351, 89, 156, 261, and 9 targets were obtained from each respective database (Table S5). The collected targets related to CC were integrated, resulting in a total of 758 CC-related targets. Finally, 125 potential protein targets for the treatment of CC were revealed using the R package "VennDiagram" (Fig. 7A).

3.8. The PPI networks

The PPI network was established by inputting 125 candidate therapeutic targets onto the STRING database. Through Cytoscape processing, a network consisting of 107 nodes and 594 edges was generated. The size and color of the nodes were indicative of their respective degree values (Fig. 7B).

The CytoNCA tool was used to analyze the topological parameters of the PPI network. This analysis identified 34 targets that were above the average (Fig. 7C). Among these targets, the top 6 were SRC (degree = 41), STAT3 (degree = 40), TP53 (degree = 39), PIK3R1 (degree = 37), MAPK3 (degree = 36), and PIK3CA (degree = 36). These core targets play a critical role in the treatment of CC. The original PPI network obtained from the STRING database is shown in Fig. S2. More detailed data regarding the CytoNCA analysis is presented in Table S6.

3.9. GO and KEGG pathway enrichment analyses

The R programming language and associated packages were employed to perform GO and KEGG enrichment analyses on 125 potential therapeutic targets. In terms of biological processes, a total of 2455 statistically significant GO items were obtained, and the results ranked by P.adjust values showed that potential therapeutic targets mainly involve gland development and oxidative stress. Similarly, a total of 52 cellar composition items were enriched, mainly in membrane rafts and membrane microdomains. A total of 146 molecular functional items were enriched, indicating that potential therapeutic targets mainly affect protein serine/threonine kinase activity and protein tyrosine kinase activity. The top ten terms for each of the three groups are shown in Fig. 8A.

Through KEGG pathway analysis, a total of 168 signaling pathways were obtained (Table S7). The top 30 significant enrichment pathways are displayed in Fig. 8B, sorted by P.adjust values. The targets were mainly enriched in the PI3K/AKT and MAPK signaling pathways, Proteoglycans, and MicroRNAs. Among them, the PI3K/AKT signaling pathway involved the most potential therapeutic targets, indicating that it may be a critical pathway for AP treatment of CC (Fig. 8C). Among the top 30 enriched pathways, targets CCND1, MAPK1, PIK3CA, PIK3R1, AKT1, AKT2, MAP2K1, RAF1, TP53 and BCL2 accounted for the largest proportion.

3.10. Construction of the "C-T-P" network diagram

To elucidate the connections between compounds, potential therapeutic targets, and the top 30 pathways, the "C-T-P" network was constructed. The three compounds in AP that exhibited the highest degree of association with potential therapeutic targets were quercetin (target number = 35), methylprednisolone (target number = 33), and caudatin (target number = 30). Fig. 9 revealed the interaction between 75 compounds, 125 targets, and 30 pathways. The lines are denser, representing that the interaction is more obvious. Which indicated the possible synergistic or antagonistic effects of AP's multi-component and multi-target nature.

3.11. Molecular docking

Core receptor target proteins, including SRC (PDB ID: 7NG7) [25], STAT3 (PDB ID: 6NJS) [26], TP53 (PDB ID: 7B4N) [27], PIK3R1 (PDB ID: 8DCP) [28], ERK1 (PDB ID: 4QTB) [29], and PIK3CA (PDB ID: 7L1C) [30], were docked with the active compounds of AP using AutoDock Vina.

The results showed that except for some acidic compounds, the docking binding energy of the other active ingredients and the core target was less than −5 kcal/mol, indicating good binding activity. Importantly, the core compounds quercetin, methylprednisolone, and caudatin have significant binding activity to the core target. Among the six core targets, quercetin exhibited the most excellent

Table 2
DEGs were identified from the three GSE datasets.

DEGs	GENE NAME
Upregulated	OSTF1, KIF14, FCER1A, TOPBP1, AXOT, DNA2, PLEKHM1, ZIC2, CLTB, KNTC1, DOCK9, ATAD2, UBL3, PARP2, ANXA1, KPNA1
Downregulated	TYMS, CRISP3, FLJ20311, ANO10, RFC4, PHYHIP, CDKN2A, MINDY1, RRP1B, SCNN1B, RNASEH2A, CRISP2, SPAG5, FAM3D, HOXC9, RBM20

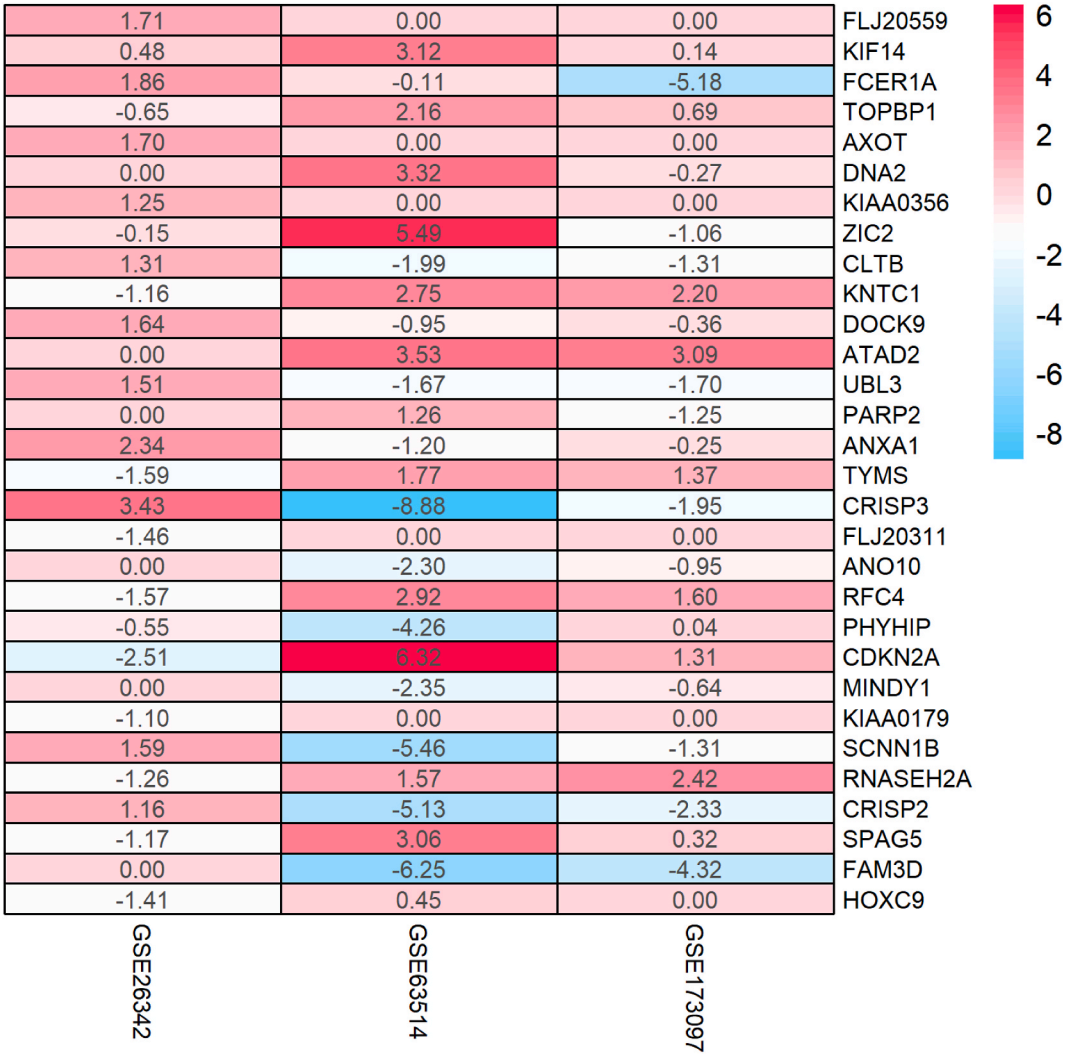

Fig. 6. Top 15 upregulated and downregulated DEGs of CC obtained by RRA analysis.

docking binding energy to MAPK3 with a value of −9.4 kcal/mol. Methylprednisolone exhibited the most excellent docking binding energy to PIK3R1 with a value of −8.5 kcal/mol, while caudatin exhibited the most excellent docking binding energy to PIK3CA with a value of −8.4 kcal/mol. Interestingly, Erionic acid E's binding activity to core targets is extremely strong and deserves further attention. It has the lowest bonding energy to SRC at −11.5 kcal/mol.

The 2D and 3D graphs of binding sites of the binding sites of quercetin, methylprednisolone, caudatin, and Erionic acid E to the core targets that bind most strongly to them were visualized by the Discovery Studio 2021 client (Fig. 10A–D). The binding energy of all docking results was presented as a heat map (Fig. 10E).

4. Discussion

Molecular networking applications are increasingly recognized for their tremendous potential in uncovering complex secondary metabolites in plants, annotating known compounds, and revealing their derivatives based on secondary mass spectrometry similarity. In this study, through UPLC-Q-TOF-MS-based non-targeted metabolomics combined with MolNetEnhancer, we found several compounds in AP, including flavonoids, alkaloids, C_{21} steroids, terpenes, organic acids and other compounds. Flavonoids are an important secondary metabolite that is widely present in plants and is essential for plant growth and development [31]. Alkaloids found plants employ unique mechanisms to protect the organisms from potential threats posed by predators and pathogens. The existence of precursor molecules, along with enzymatic reactions and chemical transformations during alkaloid conversion, leads to the development of diverse structural alterations in alkaloids [32]. Terpenoids, alternatively referred to as isoprenoids, are abundantly present in various natural products. The extensive structural and stereochemical variability exhibited by terpenoids contributes to their broad spectrum of biological functionalities [33]. The seven flavonoids identified included flavonols, isoflavonols, and their glycosides.

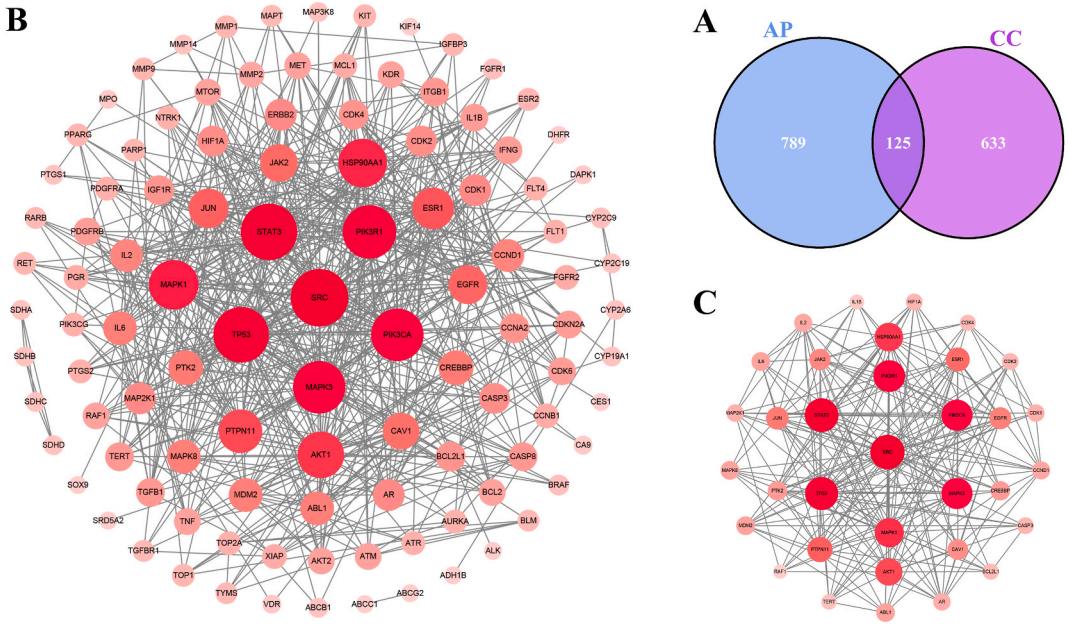

Fig. 7. (**A**) Venn diagram of potential therapeutic targets for AP against CC. (**B**) PPI networks of potential therapeutic targets. (**C**) hub targets of the PPI network.

Thereinto, Quercetin (**1**) is a particular subclass of flavonoids that is crucial in facilitating diverse physiological processes in plants [34]. Quercetin 3-*O*-β-cellobioside (**4**) has an additional cellobiose structure based on Quercetin (**1**), which has been shown to have the effect of promoting intracellular melanin synthesis [35]. Three of the 15 alkaloids identified were isoquinoline, including (6aS)-1,2,10-trimethoxy-6-methyl-6-oxido-5,6,6a,7-tetrahydro-4H-dibenzo[de,g]quinolin-6-ium-9-ol (**14**), Duguetine N-oxide (**15**) and Isocorydine (**16**). A previous study has shown Duguetine N-oxide (**15**) have strong antitumor activity against HCT-8, SF-295 and MDA/MB-435 cell lines [36]. Administration of Isocorydine (**16**) may enhance IL-6 expression in bone marrow-derived macrophages while attenuating phosphorylation of p65 and JNK, and contribute to the protection of mice against acute lung injury induced by lipopolysaccharide [37]. The remaining 12 compounds are other alkaloids, which are rare among the natural products reported in the literature, and we will further investigate them during isolation and purification.

In addition, the mechanism of action of AP in the treatment of CC was also explored based on network pharmacology and bioinformatic analysis strategies. A total of six pivotal targets including SRC, STAT3, TP53, PIK3R1, MAPK3 (ERK1), and PIK3CA were obtained which may play pivotal roles in the process of AP against CC through PPI analysis and CytoNCA topology. SRC is a type of non-receptor tyrosine kinase (NrTK) that plays a crucial role in the regulation of tumorigenesis and the advancement of cancer [38]. STAT3 is an important downstream target for c-Src, and c-Src activates STAT3 to promote tumor progression [39]. Downregulation of phosphorylated SrcY416 has been associated with growth inhibition in CC cells [40]. The signal transduction and transcriptional activator 3 (STAT3) is a confluence point for multiple cancer-related signaling pathways, which are strongly correlated with tumor progression and modulate anti-tumor immune responses [41]. Studies have shown that STAT3 was overexpressed in CC tissues and could increase autophagy in CC cells via the Bcl2-Beclin1 axis [42]. TP53 is a tumor suppressor gene that is mutated in more than half of human malignancies. Functional defects in TP53 can lead to tumor development and drug resistance [43]. Overexpression of the early oncoprotein E6/E7 produced by HPV in host cells contributed to CC development. The oncoprotein E6 can act on TP53 through the ubiquitin ligase pathway, thereby interfering with the CC cell cycle and inhibiting apoptosis [44]. Evidence has shown that the restoration of TP53 activity can induce CC cell cycle arrest and apoptosis, thereby inhibiting tumor growth [45]. PIK3R1 is a tumor suppressor encoding PI3K regulatory subunit P85α. PIK3R1 is poorly expressed in most malignancies and is associated with tumor progression and metastasis [46]. Overexpression of PIK3R1 reversed CC proliferation, migration, and invasion which were triggered by overexpression of miR-92a [47]. In addition, gene expression analysis of CC revealed that epithelial-mesenchymal transition (EMT)-related genes PIK3R1 and STAT3 are potential biomarkers and/or therapeutic targets for CC [48]. ERK1/2 is the only downstream target of MEK kinase and the most extensively studied target in the MAPK family. ERK1/2 contributes to the occurrence of metastasis of various types of cancer [49]. Previous research has revealed that zoledronic acid may inhibit the development of cancer stem cells derived from CC cells by inhibiting phosphorylated ERK1/2 [50]. In solid tumors, the mutation or amplification of PIK3CA (encoding the p110a subunit catalyzed by PI3K) is one of the most common alterations. In a whole-exome sequencing (WES) of CC cell lines, 24.6 % of tumor samples contained repeated missense mutations of activated PIK3CA exons and 42 % contained amplification of the PIK3CA gene [51]. This suggested that PIK3CA mutations or amplifications are prevalent in CC. In recent years, exploring the effect of PIK3CA mutation on the proliferation and metabolic changes of CC has become a research hotspot. For example, PIK3CA mutation has been reported to enhance the proliferation and glycolytic capacity of CC cells by activating the β-catenin/SIRT3 signaling pathway

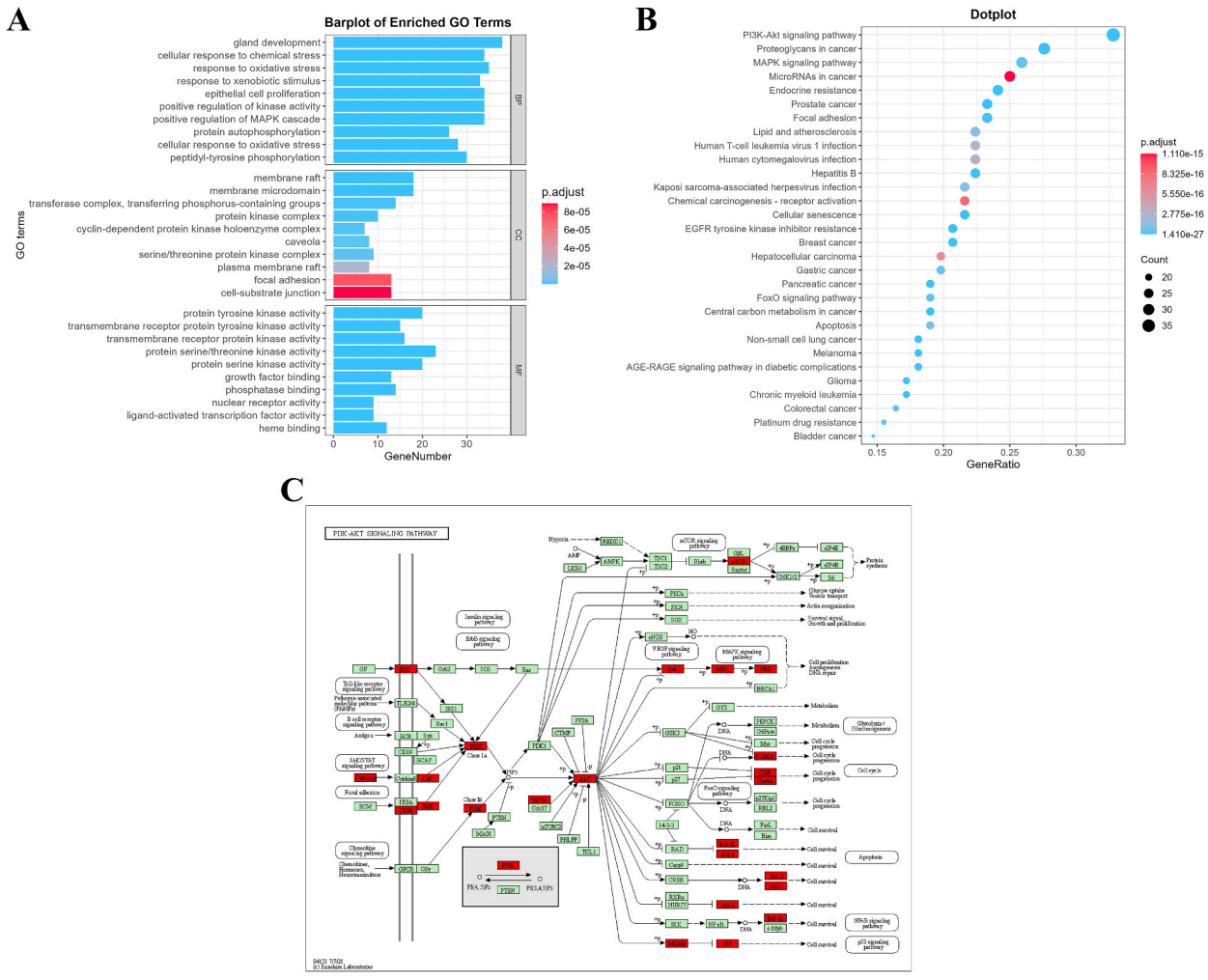

Fig. 8. GO enrichment analysis of potential therapeutic targets of AP against CC. The figure displays the top 10 terms of biological processes, cellar composition, and molecular function groups, respectively. (B) The top 30 results of KEGG pathway enrichment analysis of potential therapeutic targets of AP against CC. (C) PI3K/AKT signaling pathway diagram (Rank 1 in KEGG pathway enrichment analysis). Red nodes represented potential therapeutic targets in the PI3K/AKT signaling pathway. (For interpretation of the references to color in this figure legend, the reader is referred to the Web version of this article.)

[52]. In addition, PIK3CA mutation has been found to diminish radiosensitivity by modulating glutamine metabolism [53]. Such studies have provided new insights into treatments for CC targeting PIK3CA.

The GO analysis revealed that the potential therapeutic targets mainly involved biological processes including gland development and oxidative stress. Previous studies have shown that biomarkers of oxidative stress and antioxidants could be important markers in the diagnosis of CC [54]. The analysis of KEGG revealed that AP mainly inhibited the occurrence and development of CC through PI3K/AKT and MAPK signaling pathways. The analysis of GO revealed that the molecular function of potential therapeutic targets mainly involved protein serine/threonine kinase activity, thereby providing additional evidence for the significance of the MAPK pathway. The PI3K/AKT signaling pathway is frequently activated in a wide range of cancer types, thereby facilitating the development of tumors [55]. The Ras/Raf/MEK/ERK branch pathway is an extensively researched MAPK pathway, in which any one of the key protein function abnormalities may lead to tumorigenesis [56]. At present, molecular therapies targeting PI3K/AKT and MAPK signaling pathways are being extensively investigated for CC treatment. Preclinical studies have demonstrated that PI3K/AKT/mTOR pathway can be inhibited by Alpelisib, leading to the suppression of proliferation and migration of CC cells with PIK3CA mutations [57]. A novel polysaccharide of Rosa rugosa induced autophagy-mediated apoptosis in human CC cells primarily via the PI3K/AKT/mTOR pathway [58]. Delicaflavone from *Selaginella doederleinii* Hieron was found to induce CC HeLa cell apoptosis via the mitochondrial pathway by inhibiting the MAPK signaling pathway [59].

Active ingredients with a high degree in the C-T-P network were quercetin, methylprednisolone, and caudatin. Quercetin is a flavonoid widely present in natural products and has pronounced anticancer effects, especially against HPV-related cancers such as CC [60]. It has been reported to promote apoptosis in HeLa cells by inducing the tumor endoplasmic reticulum stress (ERS) pathway [61].

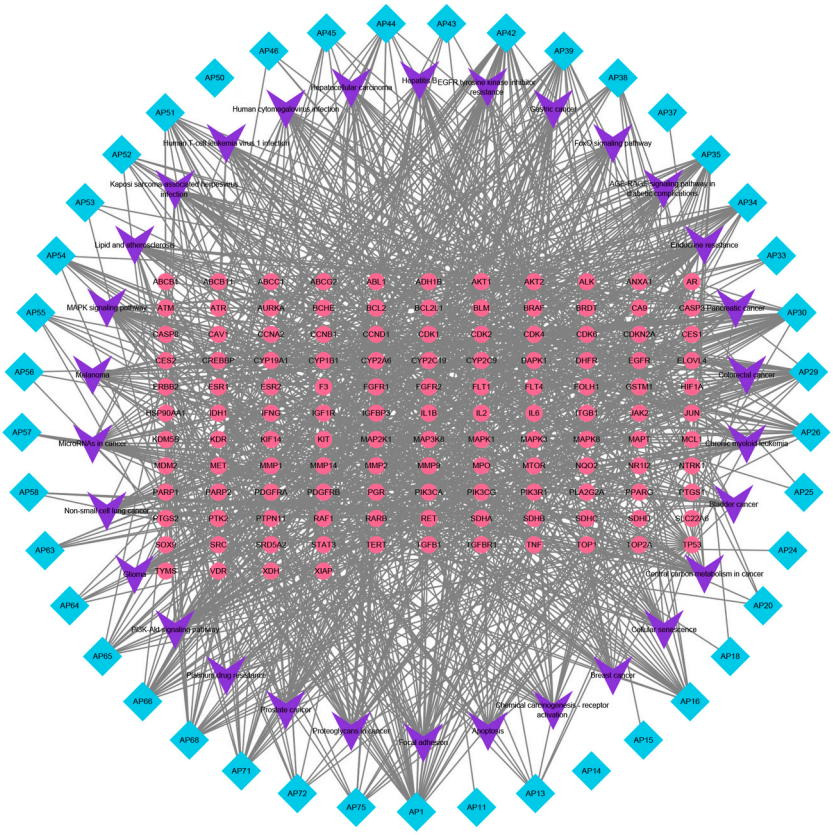

Fig. 9. Diagram of the "compound-target-pathway" network. The network consists of 198 nodes and 1380 edges, in which pink circular shapes represent the potential therapeutic targets, purple V-shaped nodes represent the signaling pathways, and blue diamond-shaped nodes represent compounds derived from AP. (For interpretation of the references to color in this figure legend, the reader is referred to the Web version of this article.)

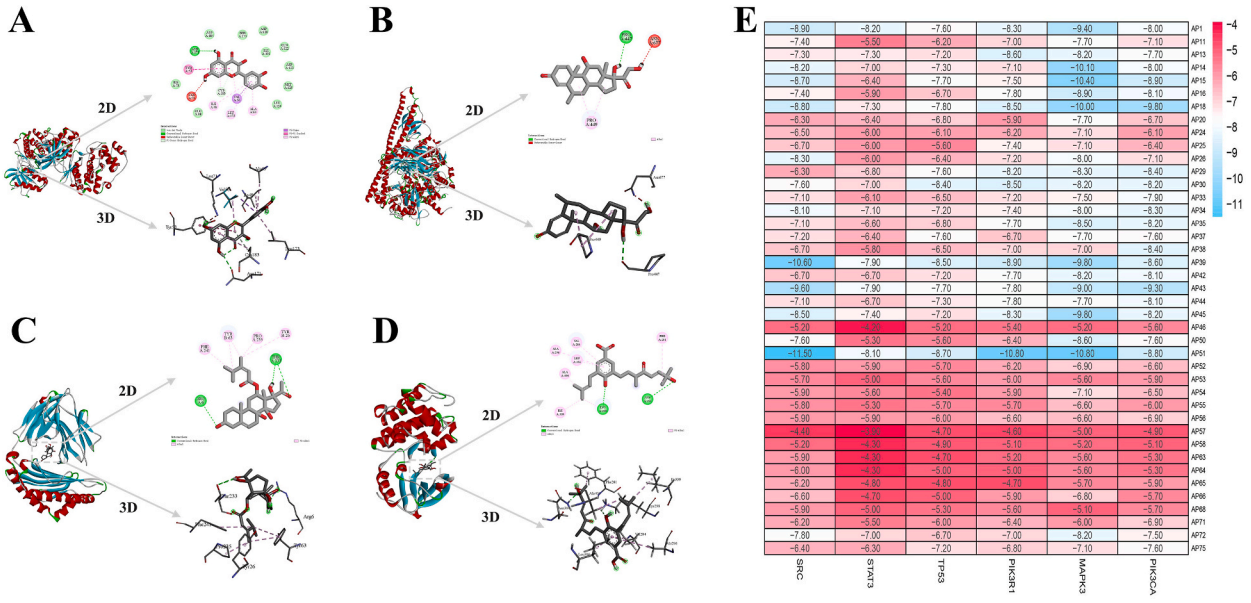

Fig. 10. The 2D and 3D schematic diagrams of molecular docking sites and heat maps of molecular docking results. (**A**) Quercetin-MAPK3; (**B**) Methylprednisolone-PIK3R1; (**C**) Caudatin-PIK3CA; (**D**) Erionic acid E-SRC; (**E**) Heatmap of docking results.

PLGA-Quercetin inhibited CC progression by activating mitochondria-dependent Caspase-3 and 7 and mitochondria-independent FoxO1 and inhibiting the PI3K/AKT pathway [62]. Methylprednisolone is a class of corticosteroids with anti-inflammatory, analgesic, immune system suppressant, and anti-allergic properties [63]. The development of cancer and its response to treatment is regulated by inflammation. Glucocorticoids can inhibit chronic inflammation in the early stages, prevent tumorigenesis, and improve the killing effect of other therapies on tumor cells [64]. Through the application of molecular docking techniques, methylprednisolone was reported to be a prospective anti-inflammatory drug for the prevention and treatment of CC [65]. Caudatin is a C_{21} steroid hormone derived from *Cynanchum auriculatum* and can arrest the cell cycle, induce apoptosis, and exert anti-tumor as well as anti-angiogenic effects. Caudatin exhibited antiproliferative and proapoptotic activity against HeLa cell lines by targeting the TNFAIP1/NF-κB signaling pathway [66].

The results of the network pharmacology analysis were further validated by conducting molecular docking experiments. The docking results demonstrated that the key compounds, namely quercetin, methylprednisolone, and caudatin, exhibited significant binding ability towards the core targets SRC, STAT3, TP53, PIK3R1, MAPK3, and PIK3CA. This suggests that the anti-CC effects of AP may primarily be attributed to the actions of quercetin, methylprednisolone, and caudatin.

Although the pharmacodynamic basis and mechanism of AP on CC were elucidated through LC-MS/MS-based molecular networking and network pharmacological strategies, this study still has some inherent limitations. Therefore, to delve deeper into the targets and mechanisms of AP in treating CC, further research involving animal or cell experiments is warranted.

5. Conclusion

In this study, 75 compounds were qualitatively identified in AP by non-targeted plant metabolomics combined with the MolNetenhancer strategy for the first time. In addition, the mechanism of action of AP in the treatment of CC was explored using network pharmacology, bioinformatics analysis, and molecular docking. We found that the main active ingredients of AP were quercetin, methylprednisolone, caudatin, among others, which can potentially regulate the signaling pathways such as PI3K/AKT and MAPK through SRC, STAT3, TP53, PIK3R1, MAPK3, PIK3CA and other targets to treat CC. This study lays the groundwork for further investigations into the anticancer properties of AP. The findings from UPLC-Q-TOF-MS analysis can serve as a roadmap for uncovering new compounds from AP, forming the basis for the search for potential antitumor lead compounds.

Data availability statement

The data that support the findings of this study are openly available in Zenodo, at https://doi.org/10.5281/zenodo.8396127.

Funding

This study was supported by Natural Science Foundation of Shandong Province (ZR2023MC009), Research Fund for Academician Lin He New Medicine (JYHL2022ZD03), College Students' Innovation and Entrepreneurship Program of Jining Medical University (cx2023069z), and National Natural Science Foundation of China (31800282).

CRediT authorship contribution statement

Hao Zhang: Conceptualization, Data curation, Methodology, Project administration, Validation, Writing – original draft, Writing – review & editing. **Ruiming Zhang:** Formal analysis, Investigation. **Yuefen Su:** Formal analysis, Investigation. **Jingrou Zheng:** Methodology, Software. **Hui Li:** Methodology, Software. **Zhichao Han:** Methodology, Software. **Yunzhen Kong:** Visualization. **Han Liu:** Visualization. **Zhen Zhang:** Resources, Visualization. **Chunmei Sai:** Conceptualization, Funding acquisition, Resources, Supervision.

Declaration of competing interest

The authors declare that they have no known competing financial interests or personal relationships that could have appeared to influence the work reported in this paper.

Appendix A. Supplementary data

Supplementary data to this article can be found online at https://doi.org/10.1016/j.heliyon.2023.e20747.

References

[1] P.A. Cohen, A. Jhingran, A. Oaknin, L. Denny, Cervical cancer, Lancet 393 (10167) (2019) 169–182, https://doi.org/10.1016/S0140-6736(18)32470-X.
[2] H. Sung, J. Ferlay, R.L. Siegel, M. Laversanne, I. Soerjomataram, A. Jemal, F. Bray, Global cancer statistics 2020: GLOBOCAN estimates of incidence and mortality worldwide for 36 cancers in 185 countries, CA Cancer J. Clin. 71 (3) (2021) 209–249, https://doi.org/10.3322/caac.21660.

[3] L. Ferrall, K.Y. Lin, R.B.S. Roden, C.F. Hung, T.C. Wu, Cervical cancer immunotherapy: facts and hopes, Clin. Cancer Res. 27 (18) (2021) 4953–4973, https://doi.org/10.3322/caac.21660.

[4] M. He, L. Xia, J. Li, Potential mechanisms of plant-derived natural products in the treatment of cervical cancer, Biomolecules 11 (10) (2021) 1539, https://doi.org/10.3390/biom11101539.

[5] S.H. Park, M. Kim, S. Lee, W. Jung, B. Kim, Therapeutic potential of natural products in treatment of cervical cancer: a review, Nutrients 13 (1) (2021) 154, https://doi.org/10.3390/nu13010154.

[6] T. Xiao, X. Cheng, J. Huang, Z. Guo, L. Tao, X. Shen, Bioactive substances inhibiting COX-2 and cancer cells isolated from the fibrous roots of *Alangium chinense* (Lour.) Harms, RSC Adv. 13 (5) (2023) 3346–3363, https://doi.org/10.1039/d2ra06931h.

[7] Y. Cai, Z. Zhou, Z.J. Zhu, Advanced analytical and informatic strategies for metabolite annotation in un-targeted metabolomics, Trends Analyt. Chem. 158 (2023), 116903, https://doi.org/10.1016/j.trac.2022.116903.

[8] M. Wang, J.J. Carver, V.V. Phelan, L.M. Sanchez, N. Garg, Y. Peng, D.D. Nguyen, J. Watrous, C.A. Kapono, T. Luzzatto-Knaan, et al., Sharing and community curation of mass spectrometry data with global natural products social molecular networking, Nat. Biotechnol. 34 (8) (2016) 828–837, https://doi.org/10.1038/nbt.3597.

[9] M. Ernst, K.B. Kang, A.M. Caraballo-Rodríguez, L.F. Nothias, J. Wandy, C. Chen, M. Wang, S. Rogers, M.H. Medema, P.C. Dorrestein, et al., MolNetEnhancer: enhanced molecular networks by integrating metabolome mining and annotation tools, Metabolites 9 (7) (2019) 144, https://doi.org/10.3390/metabo9070144.

[10] F.C. Neto, D. Raftery, Expanding urinary metabolite annotation through integrated mass spectral similarity networking, Anal. Chem. 93 (35) (2021) 12001–12010, https://doi.org/10.1021/acs.analchem.1c02041.

[11] A.T. Ramabulana, D. Petras, N.E. Madala, F. Tugizimana, Metabolomics and molecular networking to characterize the chemical space of four momordica plant species, Metabolites 11 (11) (2021) 763, https://doi.org/10.3390/metabo11110763.

[12] M. Kibble, N. Saarinen, J. Tang, K. Wennerberg, S. Mäkelä, T. Aittokallio, Network pharmacology applications to map the unexplored target space and therapeutic potential of natural products, Nat. Prod. Rep. 32 (8) (2015) 1249–1266, https://doi.org/10.1039/c5np00005j.

[13] Z. Liu, Y. Liu, G. Zeng, B. Shao, M. Chen, Z. Li, Y. Jiang, Y. Liu, Y. Zhang, H. Zhong, Application of molecular docking for the degradation of organic pollutants in the environmental remediation: a review, Chemosphere 203 (2018) 139–150, https://doi.org/10.1016/j.chemosphere.2018.03.179.

[14] P. Nhoek, S. Ahn, P. Pel, Y.M. Kim, J. Huh, H.W. Kim, M. Noh, Y.W. Chin, Alkaloids and coumarins with adiponectin-secretion-promoting activities from the leaves of orixa japonica, J. Nat. Prod. 86 (1) (2023) 138–148, https://doi.org/10.1021/acs.jnatprod.2c00844.

[15] J. Wandy, Y. Zhu, J.J.J. van der Hooft, R. Daly, M.P. Barrett, S. Rogers, Ms2lda.org: web-based topic modelling for substructure discovery in mass spectrometry, Bioinformatics 34 (2) (2018) 317–318, https://doi.org/10.1093/bioinformatics/btx582.

[16] H. Mohimani, A. Gurevich, A. Shlemov, A. Mikheenko, A. Korobeynikov, L. Cao, E. Shcherbin, L.F. Nothias, P.C. Dorrestein, P.A. Pevzner, Dereplication of microbial metabolites through database search of mass spectra, Nat. Commun. 9 (1) (2018) 4035, https://doi.org/10.1038/s41467-018-06082-8.

[17] R.R. da Silva, M. Wang, L.F. Nothias, J.J.J. van der Hooft, A.M. Caraballo-Rodríguez, E. Fox, M.J. Balunas, J.L. Klassen, N.P. Lopes, P.C. Dorrestein, Propagating annotations of molecular networks using in silico fragmentation, PLoS Comput. Biol. 14 (4) (2018), e1006089, https://doi.org/10.1371/journal.pcbi.1006089.

[18] A. Daina, O. Michielin, V. Zoete, SwissADME: a free web tool to evaluate pharmacokinetics, drug-likeness and medicinal chemistry friendliness of small molecules, Sci. Rep. 7 (2017), 42717, https://doi.org/10.1038/srep42717.

[19] A. Banik, K. Ghosh, U.K. Patil, S. Gayen, Identification of molecular fingerprints of natural products for the inhibition of breast cancer resistance protein (BCRP), Phytomedicine 85 (2021), 153523, https://doi.org/10.1016/j.phymed.2021.153523.

[20] X. Wang, W. Zhao, X. Zhang, Z. Wang, C. Han, J. Xu, G. Yang, J. Peng, Z. Li, An integrative analysis to predict the active compounds and explore polypharmacological mechanisms of Orthosiphon stamineus Benth, Comput. Biol. Med. 163 (2023), 107160, https://doi.org/10.1016/j.compbiomed.2023.107160.

[21] K.L. Mine, N. Shulzhenko, A. Yambartsev, M. Rochman, G.F. Sanson, M. Lando, S. Varma, J. Skinner, N. Volfovsky, T. Deng, et al., Gene network reconstruction reveals cell cycle and antiviral genes as major drivers of cervical cancer, Nat. Commun. 4 (2013) 1806, https://doi.org/10.1038/ncomms2693.

[22] J.A. den Boon, D. Pyeon, S.S. Wang, M. Horswill, M. Schiffman, M. Sherman, R.E. Zuna, Z. Wang, S.M. Hewitt, R. Pearson, et al., Molecular transitions from papillomavirus infection to cervical precancer and cancer: role of stromal estrogen receptor signaling, Proc. Natl. Acad. Sci. U.S.A. 112 (25) (2015), https://doi.org/10.1073/pnas.1509322112. E3255–E3264.

[23] C. Shang, J. Huang, H. Guo, Identification of an metabolic related risk signature predicts prognosis in cervical cancer and correlates with immune infiltration, Front. Cell Dev. Biol. 9 (2021), 677831, https://doi.org/10.3389/fcell.2021.677831.

[24] R. Kolde, S. Laur, P. Adler, J. Vilo, Robust rank aggregation for gene list integration and meta-analysis, Bioinformatics 28 (4) (2012) 573–580, https://doi.org/10.1093/bioinformatics/btr709.

[25] C. Temps, D. Lietha, E.R. Webb, X. Li, J.C. Dawson, M. Muir, K.G. Macleod, T. Valero, A.F. Munro, R. Contreras-Montoya, et al., A conformation selective mode of inhibiting SRC improves drug efficacy and tolerability, Cancer Res. 81 (21) (2021) 5438–5450, https://doi.org/10.1158/0008-5472.CAN-21-0613.

[26] L. Bai, H. Zhou, R. Xu, Y. Zhao, K. Chinnaswamy, D. McEachern, J. Chen, C.Y. Yang, Z. Liu, M. Wang, et al., A potent and selective small-molecule degrader of STAT3 achieves complete tumor regression in vivo, Cancer Cell 36 (5) (2019) 498–511.e17, https://doi.org/10.1016/j.ccell.2019.10.002.

[27] O. Degtjarik, D. Golovenko, Y. Diskin-Posner, L. Abrahmsén, H. Rozenberg, Z. Shakked, Structural basis of reactivation of oncogenic p53 mutants by a small molecule: methylene quinuclidinone (MQ), Nat. Commun. 12 (1) (2021) 7057, https://doi.org/10.1038/s41467-021-27142-6.

[28] J.R. Hart, X. Liu, C. Pan, A. Liang, L. Ueno, Y. Xu, A. Quezada, X. Zou, S. Yang, Q. Zhou, et al., Nanobodies and chemical cross-links advance the structural and functional analysis of PI3Kα, Proc. Natl. Acad. Sci. U.S.A. 119 (38) (2022), e2210769119 https://doi.org/10.1073/pnas.2210769119.

[29] A. Chaikuad, E.M. Tacconi, J. Zimmer, Y. Liang, N.S. Gray, M. Tarsounas, S. Knapp, A unique inhibitor binding site in ERK1/2 is associated with slow binding kinetics, Nat. Chem. Biol. 10 (10) (2014) 853–860, https://doi.org/10.1038/nchembio.1629.

[30] S.S. Chandran, J. Ma, M.G. Klatt, F. Dündar, C. Bandlamudi, P. Razavi, H.Y. Wen, B. Weigelt, P. Zumbo, S.N. Fu, et al., Immunogenicity and therapeutic targeting of a public neoantigen derived from mutated PIK3CA, Nat. Med. 28 (5) (2022) 946–957, https://doi.org/10.1038/s41591-022-01786-3.

[31] W. Liu, Y. Feng, S. Yu, Z. Fan, X. Li, J. Li, H. Yin, The flavonoid biosynthesis network in plants, Int. J. Mol. Sci. 22 (23) (2021), 12824, https://doi.org/10.3390/ijms222312824.

[32] S. Bhambhani, K.R. Kondhare, A.P. Giri, Diversity in chemical structures and biological properties of plant alkaloids, Molecules 26 (11) (2021) 3374, https://doi.org/10.3390/molecules26113374.

[33] J.D. Rudolf, T.A. Alsup, B. Xu, Z. Li, Bacterial terpenome, Nat. Prod. Rep. 38 (5) (2021) 905–980, https://doi.org/10.1039/d0np00066c.

[34] P. Singh, Y. Arif, A. Bajguz, S. Hayat, The role of quercetin in plants, Plant Physiol. Biochem. 166 (2021) 10–19, https://doi.org/10.1016/j.plaphy.2021.05.023.

[35] K. Yamauchi, T. Mitsunaga, I. Batubara, Synthesis of quercetin glycosides and their melanogenesis stimulatory activity in B16 melanoma cells, Bioorg. Med. Chem. 22 (3) (2014) 937–944, https://doi.org/10.1016/j.bmc.2013.12.062.

[36] D.B. da Silva, E.C. Tulli, G.C. Militão, L.V. Costa-Lotufo, C. Pessoa, M.O. de Moraes, S. Albuquerque, J.M. de Siqueira, The antitumoral, trypanocidal and antileishmanial activities of extract and alkaloids isolated from Duguetia furfuracea, Phytomedicine 16 (11) (2009) 1059–1063, https://doi.org/10.1016/j.phymed.2009.03.019.

[37] Y. Tu, X. Li, Y. Fu, Y. Chen, H. Fang, Y. Li, Y. Gu, J. Zhang, Isocorydine ameliorates IL-6 expression in bone marrow-derived macrophages and acute lung injury induced by lipopolysaccharide, Int. J. Mol. Sci. 24 (5) (2023) 4629, https://doi.org/10.3390/ijms24054629.

[38] X. Zhang, H. Xu, X. Bi, G. Hou, A. Liu, Y. Zhao, G. Wang, X. Cao, Src acts as the target of matrine to inhibit the proliferation of cancer cells by regulating phosphorylation signaling pathways, Cell Death Dis. 12 (10) (2021) 931, https://doi.org/10.1038/s41419-021-04221-6.

[39] L.A. Byers, B. Sen, B. Saigal, L. Diao, J. Wang, M. Nanjundan, T. Cascone, G.B. Mills, J.V. Heymach, F.M. Johnson, Reciprocal regulation of c-Src and STAT3 in non-small cell lung cancer, Clin. Cancer Res. 15 (22) (2009) 6852–6861, https://doi.org/10.1158/1078-0432.CCR-09-0767.

[40] L. Kong, Z. Deng, Y. Zhao, Y. Wang, F.H. Sarkar, Y. Zhang, Down-regulation of phospho-non-receptor Src tyrosine kinases contributes to growth inhibition of cervical cancer cells, Med. Oncol. 28 (4) (2011) 1495–1506, https://doi.org/10.1007/s12032-010-9583-3.

[41] S. Zou, Q. Tong, B. Liu, W. Huang, Y. Tian, X. Fu, Targeting STAT3 in cancer immunotherapy, Mol. Cancer 19 (1) (2020) 2145, https://doi.org/10.1186/s12943-020-01258-7.
[42] L. Wu, B. Shen, J. Li, H. Zhang, K. Zhang, Y. Yang, Z. Zu, D. Shen, M. Luo, STAT3 exerts pro-tumor and anti-autophagy roles in cervical cancer, Diagn. Pathol. 17 (1) (2022) 13, https://doi.org/10.1186/s13000-021-01182-4.
[43] Z. Wang, A. Strasser, G.L. Kelly, Should mutant TP53 be targeted for cancer therapy? Cell Death Differ. 29 (5) (2022) 911–920, https://doi.org/10.1038/s41418-022-00962-9.
[44] L. Makgoo, S. Mosebi, Z. Mbita, Molecular mechanisms of HIV protease inhibitors against HPV-associated cervical cancer: restoration of TP53 tumour suppressor activities, Front. Mol. Biosci. 9 (2022), 875208, https://doi.org/10.3389/fmolb.2022.875208.
[45] X. Zhao, W. Sun, Y. Ren, Z. Lu, Therapeutic potential of p53 reactivation in cervical cancer, Crit. Rev. Oncol. 157 (2021), 103182, https://doi.org/10.1016/j.critrevonc.2020.103182.
[46] Y. Liu, D. Wang, Z. Li, X. Li, M. Jin, N. Jia, X. Cui, G. Hu, T. Tang, Q. Yu, Pan-cancer analysis on the role of PIK3R1 and PIK3R2 in human tumors, Sci. Rep. 12 (1) (2022) 5924, https://doi.org/10.1038/s41598-022-09889-0.
[47] Y. Wang, A. Chen, C. Zheng, L. Zhao, miR-92a promotes cervical cancer cell proliferation, invasion, and migration by directly targeting PIK3R1, J. Clin. Lab. Anal. 35 (8) (2021), e23893, https://doi.org/10.1002/jcla.23893.
[48] J. Roszik, K.L. Ring, K.M. Wani, A.J. Lazar, A.V. Yemelyanova, P.T. Soliman, M. Frumovitz, A.A. Jazaeri, Gene expression analysis identifies novel targets for cervical cancer therapy, Front. Immunol. 9 (2018) 2102, https://doi.org/10.3389/fimmu.2018.02102.
[49] L. Fu, S. Chen, G. He, Y. Chen, B. Liu, Targeting extracellular signal-regulated protein kinase 1/2 (ERK1/2) in cancer: an update on pharmacological small-molecule inhibitors, J. Med. Chem. 65 (20) (2022) 13561–13573, https://doi.org/10.1021/acs.jmedchem.2c01244.
[50] L. Wang, Y. Liu, Y. Zhou, J. Wang, L. Tu, Z. Sun, X. Wang, F. Luo, Zoledronic acid inhibits the growth of cancer stem cell derived from cervical cancer cell by attenuating their stemness phenotype and inducing apoptosis and cell cycle arrest through the Erk1/2 and Akt pathways, J. Exp. Clin. Cancer Res. 38 (1) (2019) 93, https://doi.org/10.1186/s13046-019-1109-z.
[51] L. Zammataro, S. Lopez, S. Bellone, F. Pettinella, E. Bonazzoli, E. Perrone, S. Zhao, G. Menderes, G. Altwerger, C. Han, et al., Whole-exome sequencing of cervical carcinomas identifies activating ERBB2 and PIK3CA mutations as targets for combination therapy, Proc. Natl. Acad. Sci. U.S.A. 116 (45) (2019) 22730–22736, https://doi.org/10.1073/pnas.1911385116.
[52] W. Jiang, T. He, S. Liu, Y. Zheng, L. Xiang, X. Pei, Z. Wang, H. Yang, The PIK3CA E542K and E545K mutations promote glycolysis and proliferation via induction of the β-catenin/SIRT3 signaling pathway in cervical cancer, J. Hematol. Oncol. 11 (1) (2018) 139, https://doi.org/10.1186/s13045-018-0674-5.
[53] W. Jiang, X. Ouyang, Z. Ji, W. Shi, Y. Wu, Q. Yao, Y. Wang, W. Yang, L. Xiang, H. Yang, The PIK3CA-E545K-SIRT4 signaling axis reduces radiosensitivity by promoting glutamine metabolism in cervical cancer, Cancer Lett. 556 (2023), 216064, https://doi.org/10.1016/j.canlet.2023.216064.
[54] A. Shrivastava, S.P. Mishra, S. Pradhan, S. Choudhary, S. Singla, K. Zahra, L.M. Aggarwal, An assessment of serum oxidative stress and antioxidant parameters in patients undergoing treatment for cervical cancer, Free Radic. Biol. Med. 167 (2021) 29–35, https://doi.org/10.1016/j.freeradbiomed.2021.02.037.
[55] L. Yu, J. Wei, P. Liu, Attacking the PI3K/Akt/mTOR signaling pathway for targeted therapeutic treatment in human cancer, Semin. Cancer Biol. 85 (2022) 69–94, https://doi.org/10.1016/j.semcancer.2021.06.019.
[56] J. Yuan, X. Dong, J. Yap, J. Hu, The MAPK and AMPK signalings: interplay and implication in targeted cancer therapy, J. Hematol. Oncol. 13 (1) (2020) 113, https://doi.org/10.1186/s13045-020-00949-4.
[57] Y. Wei, S. Lin, W. Zhi, T. Chu, B. Liu, T. Peng, M. Xu, W. Ding, C. Cao, P. Wu, Genomic analysis of cervical carcinoma identifies Alpelisib as a therapeutic option for PIK3CA-mutant cervical carcinoma via the PI3K/AKT pathway, J. Med. Virol. 95 (3) (2023), e28656, https://doi.org/10.1002/jmv.28656.
[58] Y. Liu, H. Li, Z. Zheng, A. Niu, S. Liu, W. Li, P. Ren, Y. Liu, M. Inam, L. Guan, et al., Rosa rugosa polysaccharide induces autophagy-mediated apoptosis in human cervical cancer cells via the PI3K/AKT/mTOR pathway, Int. J. Biol. Macromol. 212 (2022) 257–274, https://doi.org/10.1016/j.ijbiomac.2022.05.023.
[59] W. Yao, Z. Lin, G. Wang, S. Li, B. Chen, Y. Sui, J. Huang, Q. Liu, P. Shi, X. Lin, et al., Delicaflavone induces apoptosis via mitochondrial pathway accompanying G2/M cycle arrest and inhibition of MAPK signaling cascades in cervical cancer HeLa cells, Phytomedicine 62 (2019), 152973, https://doi.org/10.1016/j.phymed.2019.152973.
[60] M. Ferreira, D. Gomes, M. Neto, L.A. Passarinha, D. Costa, Â. Sousa, Development and characterization of quercetin-loaded delivery systems for increasing its bioavailability in cervical cancer cells, Pharmaceutics 15 (3) (2023) 936, https://doi.org/10.3390/pharmaceutics15030936.
[61] C. He, X. Lu, J. Li, K. Shen, Y. Bai, Y. Li, H. Luan, S. Tuo, The effect of quercetin on cervical cancer cells as determined by inducing tumor endoplasmic reticulum stress and apoptosis and its mechanism of action, Am. J. Transl. Res. 13 (5) (2021) 5240–5247.
[62] N. Yadav, A.K. Tripathi, A. Parveen, PLGA-quercetin nano-formulation inhibits cancer progression via mitochondrial dependent caspase-3,7 and independent FoxO1 activation with concomitant PI3K/AKT suppression, Pharmaceutics 14 (7) (2022) 1326, https://doi.org/10.3390/pharmaceutics14071326.
[63] R. Yang, Y. Yu, Glucocorticoids are double-edged sword in the treatment of COVID-19 and cancers, Int. J. Biol. Sci. 17 (6) (2021) 1530–1537, https://doi.org/10.7150/ijbs.58695.
[64] H. Zhao, L. Wu, G. Yan, Y. Chen, M. Zhou, Y. Wu, Y. Li, Inflammation and tumor progression: signaling pathways and targeted intervention, Signal Transduct Target Ther 6 (1) (2021) 263, https://doi.org/10.1038/s41392-021-00658-5.
[65] M. Kori, K.Y. Arga, A. Mardinoglu, B. Turanli, Repositioning of anti-inflammatory drugs for the treatment of cervical cancer sub-types, Front. Pharmacol. 13 (2022), 884548, https://doi.org/10.3389/fphar.2022.884548.
[66] Z.W. Tan, S. Xie, S.Y. Hu, T. Liao, P. Liu, K.H. Peng, X.Z. Yang, Z.L. He, H.Y. Tang, Y. Cui, et al., Caudatin targets TNFAIP1/NF-κB and cytochrome c/caspase signaling to suppress tumor progression in human uterine cancer, Int. J. Oncol. 49 (4) (2016) 1638–1650, https://doi.org/10.3892/ijo.2016.3662.